Appl. Phys. B 79, 367–370 (2004)
DOI: 10.1007/s00340-004-1556-9

Applied Physics B
Lasers and Optics

A. SHEVCHENKO[1,✉]
A. JAAKKOLA[1]
T. LINDVALL[2]
I. TITTONEN[2]
M. KAIVOLA[1]

Method for obtaining high phase space density in a surface-mounted atom trap

[1] Department of Engineering Physics and Mathematics, Helsinki University of Technology, P.O.Box 2200, FIN-02015 HUT, Finland
[2] Metrology Research Institute, Helsinki University of Technology, P.O.Box 3000, FIN-02015 HUT, Finland

Received: 24 February 2004/Revised version: 7 April 2004
Published online: 11 June 2004 •

ABSTRACT We describe a method for obtaining a high phase space density of alkali atoms in a surface-mounted microscopic atom trap created above a transparent conductor or permanent magnet on a substrate prism. We show that the peak value of the phase space density can locally reach the level of $\sim 10^{-2}$ when the microtrap is loaded with atoms from a gravito-optical surface trap. Initial spin polarization of the atoms is not required.

PACS 32.80.Pj; 39.25.+k; 03.75.Be

1 Introduction

Surface-mounted atom traps are useful tools for obtaining quantum-degenerate atomic gases in samples of micrometer-scale size. These microtraps can provide tight confinement in two or three dimensions, and serve as quantum guides or dots for the trapped atoms [1–3]. This opens up perspectives for the development of integrated devices operating with matter waves. A significant advance in this direction has been the recent demonstration of Bose–Einstein condensates in traps of this kind [4–6]. The surface-mounted atom traps can also be used for fundamental studies of low-dimensional atomic gases and atom-surface interactions.

Surface-mounted microtraps are typically built on current-carrying wires that are lithographically fabricated on a planar substrate. Proposals to use permanently magnetized patterns have also been reported [2]. In the current experiments, the traps store atoms in low-field seeking magnetic states in a local minimum of a static magnetic field. The wires or permanent magnets are traditionally fabricated of materials which are opaque to light. However, there are materials which are both transparent and either conductive (as indium tin oxide) or magnetic (as iron garnets). A thin film of such material can then be deposited on a transparent substrate and subsequently patterned by using optical lithography or magnetic recording. This opens up the possibility for creating atom traps, which allow for easy access to the trapped atoms with light. If the patterns embedded into the material have the same index of refraction as the surrounding medium, one can form an evanescent-wave atom mirror on the surface and use it to cool the atoms before loading them into the microtrap. Such evanescent-wave cooling of ^{133}Cs to a temperature of a few μK has already been demonstrated in a number of experiments, using the so-called gravito-optical surface trap (GOST) [7–11].

In this work, we propose a new method for acquiring high phase space density of atoms when loading them into a surface-mounted microtrap. Starting with a sample of spin-unpolarized cold atoms in a GOST, we consider a microscopic magnetic subtrap within the GOST to be swiftly turned on in order to attract atoms in a particular magnetic substate into a lower potential. The equilibrium density in the bottom of the new trap will be dictated by the trap depth in accordance with the Maxwell–Boltzmann density distribution. With the onset of the subtrap, this density can increase by several orders of magnitude. On the other hand, by making the subtrap volume much smaller than the effective volume occupied by the whole atomic ensemble in the GOST, one can ensure the subtrap temperature remains low. This results in a strong local increase of the phase space density (see [9, 10, 12], where the subtrap is created by a tightly focused laser beam). For comparison, the techniques used to load the conventional microtraps based on current-carrying wires [4–6, 13] will transfer the whole atomic ensemble in one go into the microtrap and, consequently, no similar gain in the phase space density can occur in the loading process.

2 A microtrap on an evanescent wave

In the following, we consider a trap where the magnetic potential is created by a transparent conductor, although a permanently magnetized structure can be used as well. Let a narrow strip of conductive oxide be embedded into a thin dielectric film on the surface of a glass prism (see Fig. 1). The film can be made of, e.g., silicon nitride with the refractive index adjusted to the required value by a proper choice of the deposition conditions [14]. An evanescent-wave atom mirror can then be created above the strip through total internal reflection of a blue-detuned laser beam on the film-vacuum interface. We note that if the beam is p-polarized and incident on the film-vacuum interface at an angle close to the critical angle, the film-glass interface will only slightly affect the light transmission (by less than 1%), since the angle of incidence

✉ Fax: +358-94513155, E-mail: andrej@focus.hut.fi

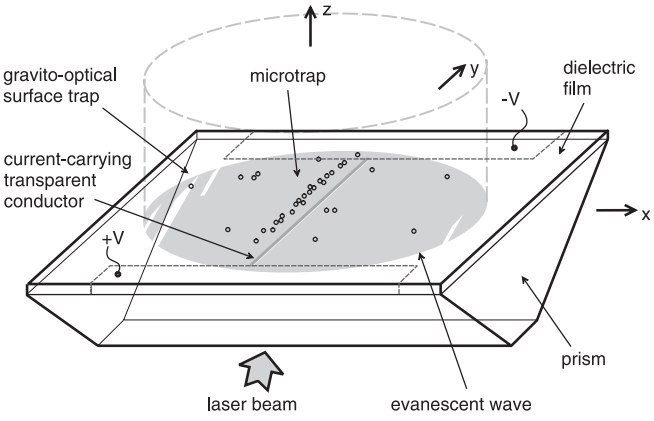

FIGURE 1 Schematic diagram for creating a microscopic atom trap above an evanescent-wave atom mirror of a gravito-optical surface trap

at this interface is close to the Brewster's angle. The potential of interaction between an alkali-metal atom and the static magnetic field and the evanescent wave reads as

$$U = \frac{1}{k_\mathrm{B}} g_\mathrm{F} m_F \mu_\mathrm{B} |\boldsymbol{B}| + \frac{\lambda_0^3}{8\pi^2 c k_\mathrm{B}} \frac{\Gamma}{\delta} I_0 \exp(-z/\Lambda)\,, \qquad (1)$$

where U is expressed in units of temperature. Here $\boldsymbol{B}$ stands for the magnetic-field induction, m_F for the projection of the total angular momentum $\boldsymbol{F}$ of the atom on the magnetic-field direction, and λ_0 and Γ for the wavelength of the D_2-line and the excited-state decay rate, respectively. The parameter k_B denotes Boltzmann's constant, g_F the Landé g-factor, μ_B the Bohr magneton, and c the velocity of light. The detuning δ of the evanescent-wave frequency from the atomic resonance is measured with respect to the lower hyperfine ground state $|G_1\rangle$ that, e.g., for ^{87}Rb, is $|5\,^2S_{1/2}, F = 1\rangle$. The quantities I_0 and Λ are the maximum value and the decay length of the evanescent-wave intensity, respectively, and z is the distance from the surface. Equation (1) has been written for an atom in a $|G_1, m_F\rangle$-state in the limit of low saturation of the atomic transition in the evanescent wave. Both gravity and the van der Waals interaction terms (see [11, 15, 16]) have been neglected, since they do not significantly affect the potential U around the potential minimum of the traps considered here. Additionally, the detuning δ is assumed to be much larger than the Zeeman energy separation of the $|G_1, m_F\rangle$-states.

As an example, we show in Fig. 2a and b the calculated potential U for ^{87}Rb in the state $|G1, m_F = +1\rangle$ (high-field seeking atoms) above a current-carrying strip located 100 nm below the surface and having a thickness of 200 nm and a width of 2 μm. The strip carries a current of 0.43 mA (the electrical resistivity of indium tin oxide, $5 \times 10^{-6}\,\Omega\,\mathrm{m}$, is appropriate for such currents). The intensity I_0 is equal to $6 \times 10^7\,\mathrm{W/m^2}$, which corresponds to the case of a totally reflected beam with a diameter of 0.6 mm and a power of 2.5 W at an incident angle of 31° ($n = 2$, as for indium tin oxide). The detuning δ and the decay length Λ are 4500 GHz (-9 nm at $\lambda_0 = 780$ nm) and 250 nm, respectively. Figure 2a shows equipotential contours in the transverse plane with a step of 2 μK. Figure 2b shows the potential U along the vertical line crossing the point of the potential minimum. The trap is 18 μK deep and has transverse dimensions on the order of a micrometer. The

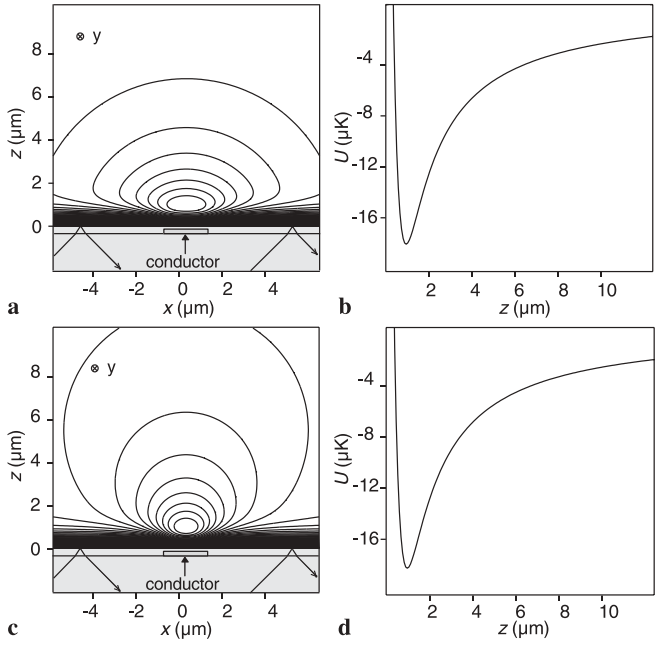

FIGURE 2 Atom traps above a current-carrying transparent wire for ^{87}Rb in high-field seeking $|G_1, m_F = +1\rangle$ state (cases **a** and **b**) and in low-field seeking state $|G_1, m_F = -1\rangle$ (cases **c** and **d**). The trap for low-field seeking atoms is obtained by applying an external magnetic field along the x axis. **a** and **c** illustrate equipotential contours of the trapping potential U with a step of ~ 2 μK. **b** and **d** show vertical cross sections of the potentials across the point of the potential minimum

distance of the potential minimum from the surface is about 1 μm. The trap size along the y-direction may be limited, e.g., by making the strip much wider outside the trapping region (see Fig. 1). On the other hand, the y-size can be adjusted by shifting the hollow beam in the direction perpendicular to the current-carrying strip. If the length of the trapping region is much larger than its transverse size, the longitudinal profile of the confining potential can be considered to be uniform in between the potential barriers at the trap ends. The trap of Fig. 2c and d for ^{87}Rb in the state $|G1, m_F = -1\rangle$ (low-field seeking atoms) is obtained by applying a bias magnetic field $\widetilde{B} = 5$ G solely along the x axis. For this trap, the point where the total magnetic field has zero strength is located below the film surface and, therefore, no Majorana spin flips can occur. For convenience, the background value of the potential U in the plots is set to 0. The trap has approximately the same depth and position above the film surface as the trap of Fig. 2a and b. However, the trapping frequency in the horizontal direction near the bottom is higher, ~ 40 kHz compared to ~ 20 kHz in the former trap. The frequency in the vertical direction is approximately the same in both traps, and it is roughly equal to 60 kHz.

The rate of optically induced transitions of atoms in the traps can be assessed by making use of the approximation of low saturation. The Zeeman splitting of the atomic energy levels can be neglected owing to the large detuning δ. The probability for an atom at rest at a certain height z to make a transition from any of the states $|G1, m_F\rangle$ is given as a function of time t by $p = 1 - \exp(-\Gamma S t/3)$, where S is the saturation parameter [11]. Defining the characteristic time for the process as $\tau_\mathrm{c} = 3/\Gamma S$, and expressing S in terms of the

z-dependent evanescent-wave intensity, one obtains

$$\tau_c = \frac{8\pi^2\hbar c}{\lambda_0^3}\left(\frac{\delta}{\Gamma}\right)^2 \frac{1}{I_0}\exp(z/\Lambda)\,. \tag{2}$$

This expression gives for the time τ_c a value of ~ 2 s in the trap center for both trap types considered above.

3 Loading of atoms into the microtrap

Let a magnetic subtrap suddenly appear within the GOST. We assume that the GOST contains 2×10^6 atoms of ^{87}Rb at temperature $T_i = 3\,\mu$K (the numbers are as in [8] and [9]), and that the effective volume of the GOST is $\Omega_{\rm GOST} = \pi(400\,\mu{\rm m})^2 \times 30\,\mu$m, where 400 μm is the GOST radius and 30 μm is the thermal height of the atomic sample above the evanescent-wave mirror. For the sake of generality, we denote the magnetic quantum states of the atoms in the lower hyperfine ground state by $|m_a\rangle$, $|m_F = 0\rangle$, and $|m_r\rangle$, where the subindices a and r denote states which are attracted and repelled by the subtrap, respectively. Thus, independently of the kind of subtrap, the trapped state is $|m_a\rangle$. The subtrap depth for this state is assumed to be $\Delta U_{\rm st} = 18\,\mu$K. After the appearance of the subtrap, the density distribution and the temperature of the atoms in the GOST will change. A new equilibrium state will be reached in a time of $\tau_{\rm eq} \simeq 0.5$ s [9]. Assuming that the atoms occupy the different magnetic states with equal probability, we calculate the final number N_a and temperature $T_{\rm f}$ of atoms in the subtrap by solving the following coupled equations

$$T_{\rm f} = \frac{1}{3}(T_a + T_0 + T_r),\ \text{where } T_0 = T_r = T_i\,, \tag{3}$$

$$T_a = T_i + \frac{2}{3}\Delta U_{\rm st}\left(\frac{N_a}{N_{\rm t}/3} - \frac{\Omega_{\rm st}}{\Omega_{\rm GOST}}\right), \tag{4}$$

$$\frac{N_{\rm t}/3 - N_a}{\Omega_{\rm GOST} - \Omega_{\rm st}} = \frac{N_a}{\Omega_{\rm st}}\exp\left(-\frac{\Delta U_{\rm st}}{T_{\rm f}}\right), \tag{5}$$

where $N_{\rm t}$ is the total number of atoms in the GOST and $\Omega_{\rm st}$ the effective volume of the subtrap. The above equations are obtained by applying the law of energy conservation, and assuming Maxwell–Boltzmann density distribution for the atoms in each of the magnetic states. For simplicity, both the GOST and the subtrap potentials are assumed to be square-wells. We also take into account the fact that the magnetic field forming the subtrap has no influence on the atoms in the state $|m_F = 0\rangle$ and only a minor influence on the repelled-state atoms. Therefore, the auxiliary variables T_0 and T_r, which are the temperatures that could be reached by the sample if the atoms were initially spin-polarized into the $|m_F = 0\rangle$ and $|m_r\rangle$ states, respectively, are equated to T_i. Thus, the redistribution of the attracted-state atoms alone is considered to contribute to the temperature change of the whole sample. By solving (3)–(5) we find the dependence of N_a and $T_{\rm f}$ on the volume $\Omega_{\rm st}$. Using these results we then calculate the density $n_0 = N_a/\Omega_{\rm st}$ and the peak phase space density $\Phi_{\rm st} = n_0(\hbar\sqrt{2\pi/Mk_{\rm B}T})^3$ in the subtrap. Figure 3 illustrates the dependence of N_a and $\Phi_{\rm st}$ on the ratio $R = \Omega_{\rm GOST}/\Omega_{\rm st}$. The values of $\Omega_{\rm st}$ are also shown in the figure. In the GOST, the volume $\Omega_{\rm st}$ has an upper limit of about $5\times10^3\,\mu{\rm m}^3$ corresponding to the case when the subtrap length is equal to the GOST diameter. Then, the number of atoms transferred into the microtrap is 5×10^4 and the phase space density is $\Phi_{\rm st} = 10^{-2}$. This value of $\Phi_{\rm st}$ is several orders of magnitude higher than what has been achieved so far in conventional magnetic microtraps without applying evaporative cooling. The final temperature $T_{\rm f}$ and the density n_0 in the case of $\Omega_{\rm st} = 5\times10^3\,\mu{\rm m}^3$ are calculated to be 3.3 μK and $1\times10^{19}\,{\rm m}^{-3}$, respectively. If the subtrap is made to be smaller, the temperature $T_{\rm f}$ turns out to be closer to its original value, and the density n_0 higher. This will result in an even higher value of $\Phi_{\rm st}$.

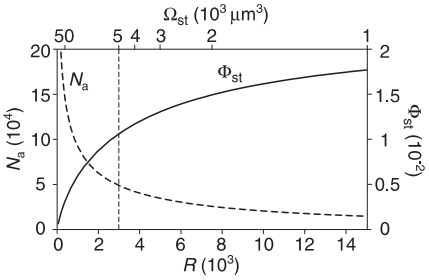

FIGURE 3 The number of atoms N_a transferred into the microtrap (*dashed line*) and the peak phase space density $\Phi_{\rm st}$ (*solid line*) versus the volume ratio $R = \Omega_{\rm GOST}/\Omega_{\rm st}$. The subtrap volume $\Omega_{\rm st}$ can not be larger than $5\times10^3\,\mu{\rm m}^3$ in the GOST considered

Owing to the low temperature that can be reached in the trap, it is easy to make the Zeeman splitting of the atomic energy levels to by far exceed the thermal atomic energy. This removes the necessity to initially spin-polarize the atoms as a way to increase the phase space density in the microtrap even in the case when more than three magnetic substates are present in the atomic ground-state manifold. Indeed, the local densities of the atoms in two neighboring magnetic states are related to each other by the constant $\kappa = \exp(-U_{\rm Z}/T)$, where $U_{\rm Z}$ is the Zeeman splitting in terms of temperature. If $U_{\rm Z} = 20\,\mu$K, as in the high-field seeker trap of Fig. 2a and b, and $T = 3.3\,\mu$K, then the factor κ is equal to 2×10^{-3}. In the low-field seeker trap, the spin polarization of the atomic sample is even better, since $U_{\rm Z}$ is on the order of 100 μK. Note also that all atoms in the other magnetic states contribute to the phase space density in the microtrap since they participate in the thermal equilibration of the atomic ensemble as a whole and, as a result, an initial spin polarization of the atoms will not bring any significant advantage.

The atoms in the microtraps are localized in a region of non-zero light intensity. However, the mean time τ_c between optical excitations of the atoms in the trap is ~ 2 s, while the time of thermalization of the atomic sample is ~ 0.5 s. Therefore, heating of the atoms in the microtrap by optical recoils can be neglected, since the rest of the atoms in the GOST will quickly thermalize the subtrap atoms. The optical transitions will nevertheless cause some loss of atoms from the microtrap. One loss mechanism is due to optical transitions to the untrapped magnetic states, such as $|G1, m_0\rangle$ and $|G1, m_r\rangle$. Another is caused by transitions of atoms to the trapped magnetic substates of the upper hyperfine ground state $|G2\rangle$ (the atoms in these states will participate in binary hyperfine-ground-state exchange collisions, which, in the case of high atomic density, will lead to a fast loss of the participants [17]). The loss rate due to the optical transitions will therefore be on

the order of $\gamma_{\rm opt} = 1/\tau_{\rm c} = 0.5\ {\rm s}^{-1}$, which is still 4 times lower than the rate of thermalization of the GOST. Taking into account the fact that the lost atoms are quickly substituted with other atoms from the GOST, we can conclude that the loss mechanisms will not significantly affect the number density and the phase space density of the atoms in the microtrap. The three-body-recombination loss rate $\gamma_{\rm 3b} = L_{\rm 3b} n_0^2$ is negligibly low for ^{87}Rb due to the small coefficient $L_{\rm 3b}$, which is on the order of $4 \times 10^{-30}\ {\rm cm}^6/{\rm s}$ [18].

4 Conclusions

We have described a novel approach for creating microscopic atom traps on a surface and a way to load them with atoms in order to obtain high phase space density. The microtrap proposed differs from the traps used in current experiments, as it is built from transparent materials. This feature makes it possible to load the trap with atoms from a gravito-optical surface trap and, in addition, to externally control the atom motion with focused laser light. The loading technique allows obtaining phase space densities close to the level of 0.01 which is a good starting point for creating, e.g., Bose–Einstein condensates. We note that a BEC of Cs atoms on a prism surface has recently been obtained, using a GOST and an all-optical subtrap [10].

The trap we propose can store atoms in either low- or high-field seeking magnetic states. In addition, if the trap is created by making use of transparent magnets, a low level of magnetic-field fluctuation could be achieved [2, 19]. A promising magnetic material could be a ferrimagnetic bismuth- and gallium-substituted iron garnet, which is essentially transparent to light at $\lambda > 600$ nm ($n \approx 2.2$) and has high coercivity and remnant magnetization. Owing to these properties, a thin film of this material can be uniformly magnetized and then the magnetization direction can be locally reversed, resulting in a creation of strong magnetic field above the magnetization-flipped pattern. Patterns with sub-micrometer widths can be realized with conventional magnetic recording methods and, what is attractive, they may be erased and rewritten at will, which allows for the same device to be used for testing different trap configurations. For loading atoms into such a permanent-magnet trap with the technique presented above, one should be able to switch the trap off while the atoms are cooled in the GOST. This can be realized with, e.g., an additional blue-detuned laser beam focused in the region of the microtrap.

ACKNOWLEDGEMENTS We acknowledge financial support from the Academy of Finland.

REFERENCES

1 J. Schmiedmayer: Eur. J. Phys. D **4**, 57 (1998)
2 R. Folman, P. Krüger, J. Schmiedmayer, J. Denschlag, C. Henkel: Adv. At. Mol. Opt. Phys. **48**, 263 (2002)
3 J. Reichel: Appl. Phys. B **74**, 469 (2002)
4 W. Hänsel, P. Hommelhoff, T.W. Hänsch, J. Reichel: Nature **413**, 498 (2001)
5 H. Ott, J. Fortagh, G. Schlotterbeck, A. Grossmann, C. Zimmermann: Phys. Rev. Lett. **87**, 230 401 (2001)
6 A.E. Leanhardt, A.P. Chikkatur, D. Kielpinski, Y. Shin, T.L. Gustavson, W. Ketterle, D.E. Pritchard: Phys. Rev. Lett. **89**, 040 401 (2002)
7 Yu.B. Ovchinnikov, I. Manek, R. Grimm: Phys. Rev. Lett. **79**, 2225 (1997)
8 M. Hammes, D. Rychtarik, B. Engeser, H.-C. Nägel, R. Grimm: Phys. Rev. Lett. **90**, 173 001 (2003)
9 M. Hammes, D. Rychtarik, H.-C. Nägel, R. Grimm: Phys. Rev. A **66**, 051 401 (2002)
10 D. Rychtarik, B. Engeser, H.-C. Nägel, R. Grimm: cond-mat/0 309 536
11 J. Söding, R. Grimm, Yu.B. Ovchinnikov: Opt. Commun. **119**, 652 (1995)
12 T. Weber, J. Herbig, M. Mark, H.-C. Nägel, R. Grimm: Science **299**, 232 (2003)
13 R. Folman, P. Krüger, D. Cassettari, B. Hessmo, T. Maier, J. Schmiedmayer: Phys. Rev. Lett. **84**, 4749 (2000)
14 E.D. Palik: *Handbook of Optical Constants of Solids* (Academic Press, New York, 1998)
15 R. Marani, L. Cognet, V. Savalli, N. Westbrook, C.I. Westbrook, A. Aspect: Phys. Rev. A **61**, 053 402 (2000)
16 Y. Colombe, D. Kadio, M. Olshanii, B. Mercier, V. Lorent, H. Perrin: J. Opt. B: Quantum Semiclass. Opt. **5**, S155 (2003)
17 S.D. Gensemer, V. Sanchez-Villicana, K.Y.N. Tan, T.T. Grove, P.L. Gould: Phys. Rev. A **56**, 4055 (1997)
18 A.J. Moerdijk, H. M.J.M. Boesten, B.J. Verhaar: Phys. Rev. A **53**, 619 (1996)
19 C. Henkel, P. Krüger, R. Folman, J. Schmiedmayer: Appl. Phys. B **76**, 173 (2003)